Journal of Thermal Analysis and Calorimetry (2019) 135:1197–1209
https://doi.org/10.1007/s10973-018-7546-7

# Experimental investigation of natural convection heat transfer characteristics in MWCNT-thermal oil nanofluid

Suhaib Umer Ilyas[1] · Rajashekhar Pendyala[1] · Marneni Narahari[2]

Received: 24 April 2018 / Accepted: 9 July 2018 / Published online: 20 July 2018


## Abstract

The carbon nanotubes are considered as one of the highest thermal conductive material which is having a variety of heat transfer applications. The suitability of carbon nanotubes in convective heat transfer is examined using multi-wall carbon nanotubes (MWCNT)-thermal oil-based nanofluids. Stable nanofluids are prepared in the concentration range of 0–1 mass% and Prandtl number range of $415 \leq Pr \leq 600$ using ultrasonication. The natural convection heat transfer behavior is studied experimentally in a vertical rectangular enclosure with aspect ratio 4. The heat transfer experiments are conducted at varying heat flux in the range of 1594–3150 W $m^{-2}$. The heat transfer coefficient, Nusselt number and Rayleigh number are estimated for MWCNT-thermal oil-based nanofluids and are compared with pure thermal oil. A significant deterioration in heat transfer coefficient is observed at higher concentrations of nanofluids. The study signifies the adverse impact on the cooling performance of MWCNT-thermal oil-based nanofluids in natural convection heat transfer, even though higher thermal conductivities are observed in nanofluids. It is found that not only thermal conductivity is essential property in heat transfer, but other thermophysical properties are also influential towards thermal management.

**Keywords** Carbon nanotube · Heat transfer · Nanofluid · Natural convection · Rectangular enclosure · Thermal oil

## List of symbols

| | |
|---|---|
| $A$ | Heat transfer area in the test cell ($m^2$) |
| AR | Aspect ratio (m) |
| $Cp$ | Specific heat capacity of cooling water (kJ $kg^{-1}$ °C) |
| $Cp_{bf}$ | Specific heat capacity of base-fluid (kJ $kg^{-1}$ °C) |
| $Cp_{nf}$ | Specific heat capacity of nanofluid (kJ $kg^{-1}$ °C) |
| $E_{h,\,max}$ | Maximum possible uncertainty for heat transfer coefficient (–) |
| $E_I$ | Maximum possible uncertainty for ammeter (–) |
| $E_{MB}$ | Maximum possible uncertainty for mass balance (–) |
| $E_T$ | Maximum possible uncertainty for temperature (–) |
| $E_V$ | Maximum possible uncertainty for voltmeter (–) |
| $g$ | Acceleration due to gravity (m $s^{-2}$) |
| $Gr$ | Grashof number (–) |
| $h$ | Heat transfer coefficient (W $m^{-2}$ °C) |
| $I$ | Current (Ampere) |
| $k_{bf}$ | Thermal conductivity of base-fluid (W $m^{-1}$ °C) |
| $k_{nf}$ | Thermal conductivity of nanofluid (W $m^{-1}$ °C) |
| $k_w$ | Thermal conductivity of the wall (W $m^{-1}$ °C) |
| $m$ | Mass flow rate of cooling water (kg $s^{-1}$) |
| $m_{bf}$ | Mass of base-fluid (kg) |
| $m_{np}$ | Mass of nanoparticle (kg) |
| $Nu$ | Nusselt number (–) |
| $Pr$ | Prandtl number (–) |
| $q$ | Heat flux (W $m^{-2}$) |
| $Q$ | Heat transfer rate (W) |
| $Q_C$ | Heat transfer rate at the cold side (W) |
| $Q_H$ | Heat transfer rate at the hot side (W) |
| $Ra$ | Rayleigh number (–) |
| $t$ | Time (s) |
| $T$ | Temperature (°C) |
| $T_{avg}$ | Average temperature (°C) |
| $T_C$ | Corrected surface temperature of the cold wall (°C) |
| $T_{C,\,out}$ | Temperature of cold wall (°C) |
| $T_H$ | Corrected surface temperature of the hot wall (°C) |
| $T_{H,\,out}$ | Temperature of hot wall (°C) |

✉ Rajashekhar Pendyala
rajashekhar_p@utp.edu.my

[1] Chemical Engineering Department, Universiti Teknologi PETRONAS, 32610 Seri Iskandar, Perak Darul Ridzuan, Malaysia

[2] Fundamental and Applied Sciences Department, Universiti Teknologi PETRONAS, 32610 Seri Iskandar, Perak Darul Ridzuan, Malaysia

$T_{in}$ Temperature of cooling water inlet (°C)
$T_{out}$ Temperature of cooling water outlet (°C)
$V$ Voltage (V)
wt.fr Weight fraction of nanoparticles in nanofluid (–)
$x$ Position of the thermocouples (m)
$x_w$ Thickness of the wall (m)

### Greek symbols

$\beta$ Coefficient of thermal expansion (1/°C)
$\beta_{bf}$ Coefficient of thermal expansion of base-fluid (1/°C)
$\beta_{nf}$ Coefficient of thermal expansion of nanofluid (1/°C)
$\beta_{np}$ Coefficient of thermal expansion of nanoparticle (1/°C)
$\varphi_P$ Weight fraction of nanoparticles (–)
$\varphi_v$ Volume fraction of nanoparticles (–)
$\rho$ Density (kg $m^{-3}$)
$\rho_{bf}$ Density of base-fluid (kg $m^{-3}$)
$\rho_{nf}$ Density of nanofluid (kg $m^{-3}$)
$\rho_{np}$ Density of nanoparticle (kg $m^{-3}$)
$\mu$ Viscosity (Pa s)
$\mu_{bf}$ Viscosity of base-fluid (Pa s)
$\mu_{nf}$ Viscosity of nanofluid (Pa s)
$\delta$ Distance between hot and cold walls (m)

## Introduction

The cooling characteristics of heat transfer processes are highly dependent on the thermophysical properties of thermal fluids in the system. The thermal fluids are utilized in variety of industries particularly in microelectronics, nuclear cooling, solar collectors, power generation, distributor transformer heat exchangers, air conditioning, and engine cooling. The conventional thermal fluids are not favorable for heat transfer due to weak thermal properties and extensive progress is required for the preparation and utilization of upgraded thermal fluids for advanced heat-transfer applications. The addition of nanoparticles in conventional thermal fluids for the improvement in thermal properties can be an exquisite choice for the optimal and economical thermal management of heat-transfer processes. The unique thermal, chemical and mechanical properties of nanoparticles tend towards the preparation of different combinations of nanofluids for many applications other than heat transfer such as pharmaceuticals, food processing, crystal growth, fuels, and lubricants [1–4].

Extensive studies are found on the improved effective thermal conductivity of nanofluids [5]. However, the thermal conductivity solely cannot define the heat transfer improvement in heat transfer processes. The addition of nanoparticles in conventional base-fluids alters other thermophysical properties such as density, viscosity, specific heat capacity and coefficient of thermal expansion. It is noteworthy that most of the industrial thermal management is carried out using convective heat transfer processes [6]. In convective heat transfer processes, all of the aforementioned effective properties play a significant role. The increase in effective density and effective viscosity of nanofluids can deteriorate the heat transfer performance. Other than these, the stability of nanofluids is an important aspect for the efficient utilization of nanofluids in various applications. Extensive studies on the stability of nanofluids are found and researchers have managed to stabilize different types of nanoparticles in conventional liquids using mechanical and chemical techniques [7–9].

Carbonaceous nanoparticles are known for their highest thermal conductivities especially carbon nanotubes (CNT). There are many studies reporting the improvement of effective thermal conductivity in the colloidal dispersions of CNT-water- and CNT-oil-based nanofluids. Limited experimental investigations are found on the natural convective heat transfer performance of CNT-based nanofluids. Natural convection heat transfer process depends on the buoyancy-driven forces which can be significantly affected by the increase in effective viscosity and effective density of working fluid [10].

Natural convection heat transfer behavior in nanofluids has been theoretically studied widely in different geometries and scenarios [11–17]. However, few experimental investigations are reported on the natural convection in nanofluids [18]. A few studies have pointed out the significant difference between theoretical and experimental investigations [19]. Hu et al. [20] investigated natural convection behavior of alumina-water-based nanofluids in square enclosure experimentally and theoretically. The low concentration of nanofluids (1 mass%) showed better Nusselt number values as compared to high concentrations of nanofluids (2–3 mass%). They termed effective thermal conductivity as an advantageous factor and effective viscosity as a disadvantageous factor for heat transfer improvement using nanofluids. Mahrood et al. [21] investigated the natural convection behavior in $TiO_2$- and $Al_2O_3$- carboxymethyl cellulose/water-based non-Newtonian nanofluids. The lower concentrations ($\leq 0.2$ vol%) showed incremental Nusselt number. However, the values of Nusselt number decreased in higher concentrations of nanofluids.

Li et al. [22] investigated the natural convection behavior in ZnO-ethylene glycol/water-based nanofluids based on experimentally measured thermophysical properties. It was found that the heat transfer coefficient of nanofluids increases with an increase in heating power in the enclosure. It was also observed that the nanofluids with higher percentage of ethylene glycol exhibited poor heat transfer performance. The reason was attributed to the

higher thermal resistance caused by ethylene glycol. Beheshti et al. [23] experimentally the investigated natural convection heat transfer behavior in low concentrations of 0.001 and 0.01 mass% multi-wall carbon nanotubes (MWCNT)-transformer oil-based nanofluids at input power range of 50–150 W. The Nusselt number and heat transfer coefficient were found to be increasing with nanotube concentration. Amiri et al. [24] experimentally studied the natural convection behavior in hexylamine coated MWCNT-transformer oil-based nanofluids. Two different concentrations of nanofluids, 0.001 and 0.005 mass%, were investigated in a transformer reservoir model. It was found that heat transfer coefficient increased with an increase in nanotube concentration and input power.

Thomas et al. [25] investigated the cooling behavior of boron nitride-mineral oil-based nanofluids. The natural convection behavior was studied in a lumped system where a copper test piece was heated up to a known temperature and then dipped inside the nanofluid originally at room temperature. The temperature transients of the copper test piece were compared with the pure oil and it was found that the nanofluids did not have any significant effect on the cooling performance. The heat transfer coefficient of nanofluids was found to be slightly lower than pure oil. Heris et al. [26] experimentally investigated the natural convection in an inclined cavity using CuO-, $TiO_2$-, $Al_2O_3$-turbine oil-based nanofluids. It was reported that the Nusselt number of pure oil was found to be higher than nanofluids for all inclination angles. It was found that the $TiO_2$-based nanofluids comparably exhibited higher Nusselt number than other nanofluids for all concentrations. Table 1 presents the natural convection behavior of different nanofluids in different geometries.

Many studies have reported the incremental effective thermal conductivity of carbon nanotubes-based nanofluids [35]. However, the performance of high concentrations of carbon nanotubes-based nanofluids during natural convection heat transfer process at varying particle loading are not found in literature. Very few studies are found on the natural convection heat transfer behavior in oil-based nanofluids. In a recent study [18], functionalized alumina ($f$-$Al_2O_3$)-thermal oil-based nanofluids were used to investigate the natural convection heat transfer behavior in a vertical rectangular enclosure. Whereas, in the present work, MWCNT-thermal oil-based nanofluids with different nanotube concentrations are employed to analyze heat transfer characteristics, which implies the novelty of the present work. The present work aims to address the aforementioned deficit in the existing literature and there is a need to study and characterize the heat transfer behavior of different combinations of nanofluids. The natural convection behavior of nanotubes-based nanofluids is investigated at high concentrations (up to 1 mass%). The experimentally measured thermophysical properties are used to estimate heat transfer characteristics. The thermophysical properties are taken from Ilyas et al. [36]. The suitability of CNT-thermal oil-based nanofluids for convective heat transfer processes is investigated at a fixed aspect ratio of 4 and different input heat fluxes.

## Materials

The nanofluid is comprised of multi-walled carbon nanotubes and thermal oil. The acquired MWCNTs (US Research Nanomaterials Inc., USA) are having high purity with a carbon content of $> 97$ mass%. The inner and outer diameters of the nanotubes are in the range of 5–12 and 30–40 nm, respectively. The length of the MWCNTs is in the range of 10–20 μm. The scanning electron microscopy (SEM) image of the nanotubes is shown in Fig. 1a. The transmission electron microscopy of a single nanotube with multi-walls is shown in Fig. 1b. The base-fluid, thermal oil, is a paraffinic type (C15–C50) of refined mineral oil with a purity of up to 99 mass%. The thermophysical properties of nanotubes and thermal oil are given in Table 2 [36].

## Preparation and stability of nanofluids

The nanofluids are prepared in variety of concentrations ranging from 0 to 1 mass%. The researchers have reported different chemical and mechanical mixing techniques to stabilize nanofluids [37]. However, in the current work, the stability of MWCNT-thermal oil-based nanofluids is achieved by using only mechanical mixing technique (ultrasonication). An ultrasonic homogenizer (Biologics Inc., 150 V/T) is used to mechanically stabilize nanotubes in thermal oil. The ultrasonicator is operated at 20 kHz frequency. The ultrasonication operation is applied for 45 min at 30% pulse and 70% power for each nanofluid sample. The sedimentation analysis is carried out and none of the nanofluids showed sediment for at least a month, the details are discussed in Ilyas et al. [36]. After 1 month, slight flocculated-type sediment [38] is observed in low concentrations of nanofluids, shown in Fig. 2a. The higher concentrations of nanofluids exhibited remarkable stability and nanotubes are found to be stable. The better stability at high concentrations of nanofluid is attributed to the entanglement behavior of MWCNTs in thermal oil, which causes significant increase in the viscosity. Due to this increment in the viscosity at higher concentration, the dispersion of nanotubes in oil becomes prodigious as compared to lower concentration of nanotubes in thermal oil. The particle size distribution analysis is carried out for 0.1 mass% of nanofluids is shown in Fig. 2b [36]. It is

**Table 1** Experimental studies on the natural convection heat transfer in different nanofluids

| Researcher | Geometry | Nanoparticle | Base-fluid | Parameters | Remarks |
|---|---|---|---|---|---|
| Putra et al. [27] | Cylindrical cell | $Al_2O_3$ and CuO | Water | $AR = 0.5, 1$<br>$\varphi_v = 1\%, 4\%$<br>$10^7 \leq Ra \leq 10^9$ | The Nusselt number decreases with the increase in particle concentration |
| Ho et al. [28] | Square enclosure | $Al_2O_3$ | Water | $0 \leq \varphi_v(\%) \leq 4$ | The heat transfer increment was found at low concentration (0.1 vol%) nanofluids. |
| Kouloulias et al. [29] | Rectangular enclosure | $Al_2O_3$ | Water | $125 \leq Q(W) \leq 175$<br>$0 \leq \varphi_v(\%) \leq 0.12$<br>$2.5 \times 10^9 \leq Ra \leq 5.2 \times 10^9$ | The heat transfer coefficient decreased with the increase in nanoparticle loading. |
| Wen and Ding [30] | Horizontal cylinder | $TiO_2$ | Water | $0 \leq \varphi_v(\%) \leq 1$<br>$10^4 \leq Ra \leq 10^6$ | The deterioration in heat transfer increased with nanoparticle concentration |
| Nnanna [31] | Rectangular enclosure | $Al_2O_3$ | Water | $0 \leq \varphi_v(\%) \leq 8$<br>$9.16 \leq Q(W) \leq 120.91$ | The Nusselt number showed improvement for low concentration of nanofluids ($\leq 2\%$). |
| Ni et al. [32] | Cylindrical cell | $Al_2O_3$ | Water | $\varphi_v = 0.01\%, 0.1\%$<br>$2.6 \times 10^8 \leq Ra \leq 7.7 \times 10^9$ | The heat transfer coefficient and Nusselt number decreased with an increase in nanoparticle concentration |
| Li and Peterson [33] | Rectangular enclosure | $Al_2O_3$ | Water | $0 \leq \varphi_v(\%) \leq 6$ | The natural convection deteriorated in nanofluids due to thermophoretic motion of nanoparticles |
| Choudhary and Subudhi [34] | Rectangular enclosure | $Al_2O_3$ | Water | $0 \leq \varphi_v(\%) \leq 6$<br>$0.3 \leq AR \leq 2.5$ | Higher concentration of nanofluids exhibited deterioration in heat transfer |

found that the average agglomerate size of the nanofluid did not exceed $\sim$ 250 nm after applying ultrasonication.

## Thermophysical properties of nanofluids

The thermophysical properties of nanofluids are experimentally measured and the detailed discussion can be found in the previous study [36]. It is known from many aforementioned studies, in most cases, the theoretical models do not predict thermophysical properties with precision. The aim of this study is to apply experimentally measured thermophysical properties for the analysis of heat transfer characteristics of nanofluids. The correlations based on the experimentally measured thermophysical properties of MWCNTs-thermal oil-based nanofluids are tabulated in Table 3. These correlations are used in the calculation of Nusselt number, average heat transfer coefficient and Rayleigh number. The effective density of MWCNT-thermal oil-based nanofluids was found to be closely following the theoretical model [36]. The model was proposed by Pak and Cho [39], given in Eq. 1. The model is based on the volumetric concentrations to predict effective density of nanofluids. Therefore, a conversion equation is used, given in Eq. 2. The correlations for other thermophysical properties, i.e., effective viscosity, effective thermal conductivity, effective specific heat capacity

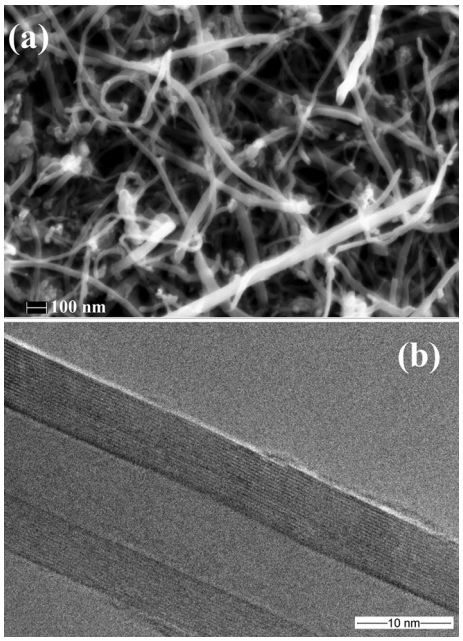


**Fig. 1** **a** Scanning electron microscopy 1(SEM); **b** transmission electron microscopy image of MWCNT

**Table 2** The properties of MWCNTs and paraffinic thermal oil

| Properties | MWCNT | Thermal oil |
|---|---|---|
| Density (kg $m^{-3}$) at 15 °C | ~ 2100 | 854.5 |
| Viscosity ($m^2$ $s^{-1}$) at 40 °C | – | $4 \times 10^{-5}$ |
| Thermal conductivity (W $m^{-2}$ °C) at 35 °C | ~ 2000 | 0.133 |
| Specific heat capacity (kJ $kg^{-1}$ °C) at 45 °C | 0.733 | 1.97 |

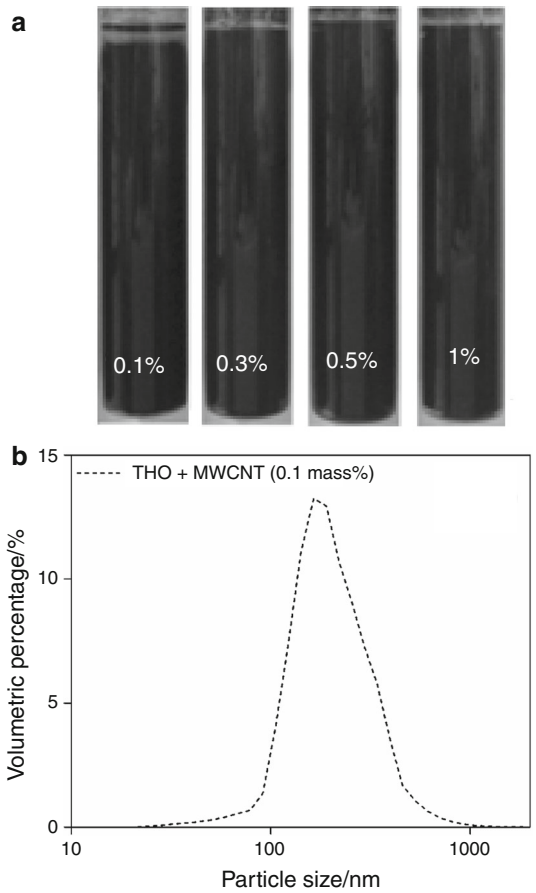


**Fig. 2** **a** The visual sedimentation analysis of nanofluids after 1 month; **b** particle size distribution of 0.1 wt % MWCNT-thermal oil- based nanofluid. Reproduced with permission from [36]

and effective coefficient of thermal expansion are tabulated in Table 3 [36].

$$\rho_{nf} = \varphi_v \rho_{np} + (1 - \varphi_v)\rho_{bf} \quad (1)$$

$$\varphi_v = \frac{m_{np}/\rho_{np}}{m_{np}/\rho_{np} + m_{bf}/\rho_{bf}} \quad (2)$$

The thermophysical properties of the nanofluids play a vital role in heat transfer improvement [40]. It is notable that all thermophysical properties change with respect to the change in nanoparticle concentration; however, significant or insignificant. The improvement in effective thermal conductivity of nanofluids is the only advantageous scenario for natural convective heat transfer [41]. The relative changes in thermophysical properties of MWCNT-thermal oil-based nanofluids at 30 °C and different particle loadings are shown in Fig. 3. It is observed that the relative changes in effective density and effective coefficient in thermal expansion are insignificant. The maximum reduction in effective coefficient of thermal expansion is observed to be 1.06% at 1 mass% concentration of MWCNT in thermal oil. The effective density of nanofluids is observed to be increased slightly up to 0.66% at 1 mass% MWCNT in thermal oil. The maximum increment in effective thermal conductivity is found to be 18.6% at 30 °C. A disagreement in the incremental effective thermal conductivity of nanotubes-oil-based nanofluids at different particle loadings was found in the literature [36, 42]. The effective viscosity of the nanofluids is observed to be increasing massively with the addition of nanotubes. The maximum increase is observed to be 62.22% at 1 mass% nanotube loading. The increment in viscosity of nanofluids was reported in many studies [43]. The relative changes in effective specific heat capacity are observed at different nanotube loadings and a maximum decrement of 12.62% is found. Similar trends were found in previous studies [28, 44].

## Experimental setup and procedure

### Natural convection setup

The natural convection heat transfer behavior in MWCNT-thermal oil-based nanofluids at various nanotube concentrations is investigated in a vertical rectangular enclosure. The aspect ratio of the enclosure is 4. The natural convection test cell with inner dimension of 12 × 4 × 3 cm is fabricated by stainless steel (SS304). The wall thickness of the hot and cold sides of the test cell is 2 mm while other walls have a thickness of 4 mm. A mica-strip heater (100 W) of 4 mm thickness and dimensions of 12 cm × 4 cm is attached to the hot wall, shown in Fig. 4 [18]. The heater is used to supply uniform heat flux at the hot-side. The cooling wall is attached to a cooling jacket. A constant flow rate of cooling water from the thermostatic bath is used to dissipate heat from the test cell. The type-K thermocouples are attached to the hot wall (TC1 and TC2) and

**Table 3** The correlations for the effective thermophysical properties of MWCNT-thermal oil-based nanofluids [36]

| Properties | Parameters | Correlations |
|---|---|---|
| Effective viscosity (Pa s) | $25 \le T(^{\circ}\mathrm{C}) \le 80$<br>$0.99 \le 1-\varphi_{\mathrm{P}}(\mathrm{wt.fr}) \le 1$<br>$\gamma(\mathrm{s}^{-1}) = 100$ | $\mu_{\mathrm{nf}} = -1.8231 - \frac{0.0686}{T} + 1.7235(1-\varphi_{\mathrm{P}}) + 3.329(1-\varphi_{\mathrm{P}})^2 + 136.7838\frac{(1-\varphi_{\mathrm{P}})^2}{T^2} - 3.2363(1-\varphi_{\mathrm{P}})^3 - 2347.39\frac{(1-\varphi_{\mathrm{P}})}{T^3}$ |
| Effective thermal conductivity (W $\mathrm{m}^{-2}$ °C) | $25 \le T(^{\circ}\mathrm{C}) \le 63.15$<br>$0.99 \le 1-\varphi_{\mathrm{P}}(\mathrm{wt.fr}) \le 1$ | $k_{\mathrm{nf}} = 0.595 - 0.4547(1-\varphi_{\mathrm{P}}) + T\left[0.7422 - 0.606(1-\varphi_{\mathrm{P}}) + \frac{0.2759}{(1-\varphi_{\mathrm{P}})} - \frac{0.3943}{(1-\varphi_{\mathrm{P}})^2}\right]$ |
| Effective specific heat capacity (kJ $\mathrm{kg}^{-1}$ °C) | $44 \le T(^{\circ}\mathrm{C}) \le 80$<br>$0.99 \le 1-\varphi_{\mathrm{P}}(\mathrm{wt.fr}) \le 1$ | $Cp_{\mathrm{nf}} = -20 + 21.573(1-\varphi_{\mathrm{P}}) - 0.012T + 0.024T(1-\varphi_{\mathrm{P}})$ |
| Effective coefficient of thermal expansion (1/°C) | $20 \le T(^{\circ}\mathrm{C}) \le 60$<br>$0.99 \le 1-\varphi_{\mathrm{P}}(\mathrm{wt.fr}) \le 1$ | $\beta_{\mathrm{nf}} = 7.56\times10^{-4} + 6.34\times10^{-7}T - 8.09\times10^{-4}\varphi_{\mathrm{P}}$ |

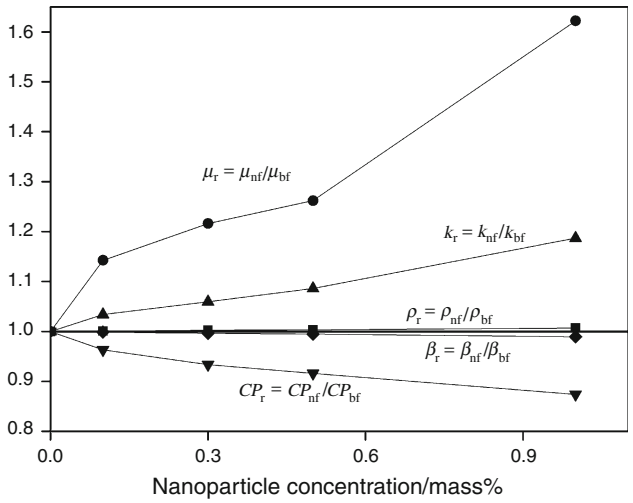


**Fig. 3** The relative changes in effective thermophysical properties of MWCNT-thermal oil-based nanofluids at 30 °C

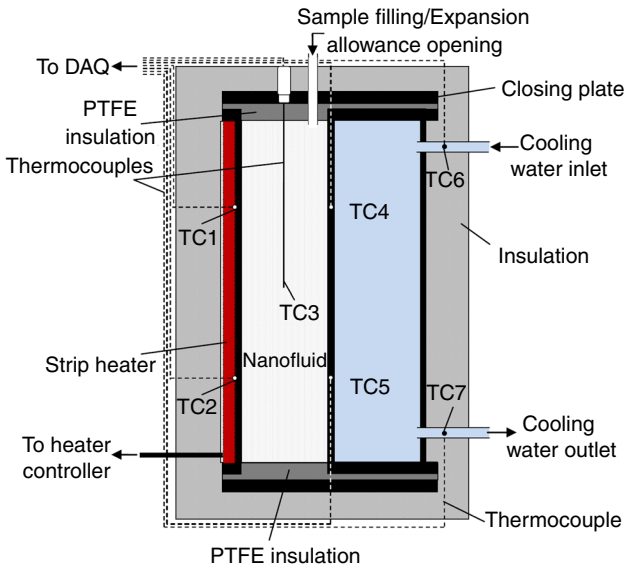


**Fig. 4** The natural convection test cell with heater and cooling jacket. Reproduced with permission from [18]

cold walls (TC4 and TC5) to measure the temperatures. At hot-side, the thermocouples (TC1 and TC2) are attached in between the mica-strip and the hot wall. At cold-side, the thermocouples (TC4 and TC5) are inserted in the holes at the middle of the cooling wall. The fluid temperature is measured at the middle of the enclosure using a type-K probe-thermocouple (TC3) of length 6 cm and thickness 1 mm. The two thermocouples are used to measure the cooling water inlet and outlet temperatures to estimate the heat output from the test cell. Teflon (PTFE) sheets are used at the top-end and the bottom-end of the enclosure to avoid leakage and provide insulation. A layer of insulating sheet (Armaflex 3.2 cm) is wrapped around the test cell to prevent heat loss.

The mica-strip heater is connected with a heater-control setup, shown in Fig. 5. The heater-control setup is powered by single-phase AC and consists of a temperature-controller, shut-down safety switch, voltmeter and voltage regulator. The current is measured by AC clamp meter. The input heat flux at the hot-side of the enclosure is controlled by the voltage regulator. At the cooling-side, the cooling water inlet and outlet streams are connected to the thermostatic bath, Hahnshin HS 3005 N, which operates at constant flow rate. The thermocouples are attached to the 8-channel data acquisition system (USB-TC, Measurement Computing Co.) to record temperature transients using a computer. For all readings, the temperature transient measurements are set for 1 Hz and it is observed that the signal noise does not surpass ± 0.05 °C.

## Data reduction

The power input at the hot-side is calculated using Eq. 3. The heat-out from the test cell at the cooling-side is calculated using Eq. 4. The heat loss is calculated for each heat transfer experiment by taking the difference between the heat-input to the hot wall ($Q_H$) and the heat-out from the cooling-side ($Q_C$). It is found that the average heat loss does not surpass 3.5% at steady-state condition.

$$Q_H = VI\cos(\alpha) \tag{3}$$

$$Q_C = mC_P(T_{out} - T_{in}), \tag{4}$$

where $\cos(\alpha)$ is the power factor for the current facility and a value of 0.9 is used for the single-phase AC-supply. The $m$ and $C_P$ represent the mass flow rate and the specific heat capacity of the cooling water, respectively. The inlet and outlet temperature of the cooling water is denoted by $T_{in}$ (TC6) and $T_{out}$ (TC7), respectively. It is illustrated from Fig. 4 that the thermocouples are attached at the outer section of the hot wall. Similarly for cooling wall, the thermocouples are inserted in the middle of the cold wall. Therefore, the corrected surface temperatures at the hot wall and cold wall boundary are calculated. The corrected surface temperatures of the hot wall $T_H$ and cold wall $T_C$ are calculated using Eqs. 5 and 6, respectively.

$$T_H = T_{H,out} - \frac{q\Delta x_w}{k_w} \tag{5}$$

$$T_C = T_{C,out} + \frac{q\Delta x_w}{2k_w}, \tag{6}$$

where $T_{H,out}$ and $T_{C,out}$ represent the average of the hot-side wall thermocouple (TC1 and TC2) measurements and average of the cold-side thermocouple (TC3 and TC4) measurements, respectively. The $q$, $k_w$ and $\Delta x_w$ represents the input heat flux, thermal conductivity of the wall material (SS304) and the thickness of the wall, respectively. The heat transfer coefficient and the Nusselt number is calculated using Eqs. 7 and 8.

$$h = \frac{Q}{A(T_H - T_C)} \tag{7}$$

$$Nu = \frac{h\delta}{k}, \tag{8}$$

where $A$, $\delta$ and $k$ represent the heat transfer area, the distance between hot and cold wall, and the thermal conductivity of the liquid in the test section, respectively. The values of $A$ and $\delta$ are constant and corresponds to 48 $cm^2$ and 3 cm, respectively. The Rayleigh number is calculated for the pure oil and nanofluids at varying nanoparticle concentration $\varphi_P$ and $\Delta T$, given in Eq. 9. The Rayleigh number is dependent on the Grashof number $Gr$ and Prandtl number $Pr$. The $Gr$ represents the ratio of buoyancy to the viscous forces while the $Pr$ represents the ratio of momentum diffusivity to thermal diffusivity.

$$Ra = Gr \cdot Pr = \frac{gq\beta\rho^2 C_P\delta^3}{hk\mu} \tag{9}$$

The heat transfer characteristics ($Nu$,$Gr$ and $Pr$) are calculated at the average temperature $T_{avg}$ of thermophysical properties. The $T_{avg}$ is given in Eq. 10.

$$T_{avg} = \frac{T_H + T_C}{2} \tag{10}$$

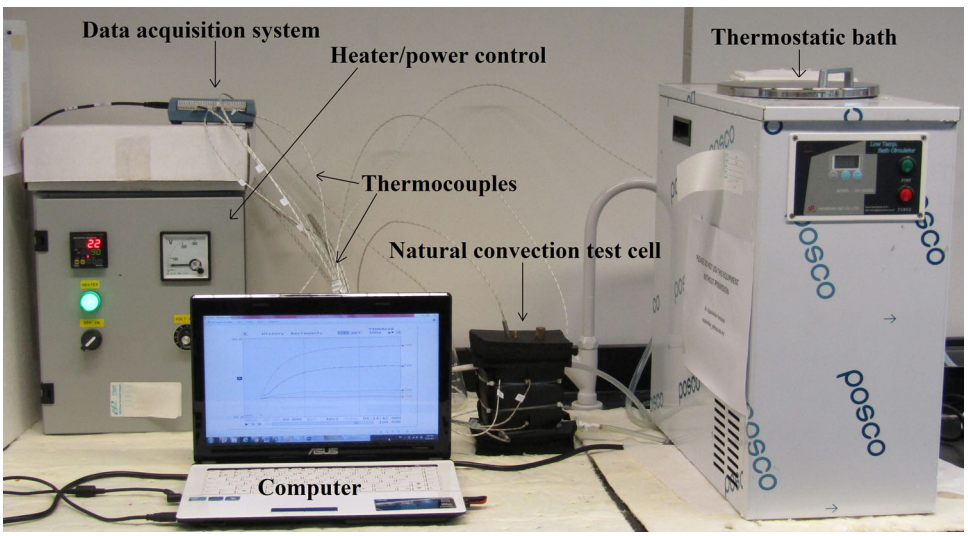


**Fig. 5** The natural convection heat transfer experimental setup

## Results and discussion

### Temperature transients

The liquid is filled inside the test cell from the top and the sample filling tube is kept open for the provision of thermal expansion of liquid. A uniform heat flux is applied at the hot-side. The investigations are carried out at five different heat flux in the range of 1594–3150 W $m^{-2}$. The same heat flux is applied to all samples for comparison purpose. The temperature transients are recorded until a steady-state condition is achieved. At initial condition, the temperature is at room temperature for the hot wall, cold wall, and the liquid filled inside the enclosure. As the power switch is turned on, the voltage is controlled to apply uniform heat flux at the hot-side. An increase in temperature is observed for the hot wall and the liquid sample inside the enclosure, shown in Fig. 6. At the cold-side, a cooling jacket is used to dissipate heat from the test cell by constant flow rate of water. A slight increase in temperature of the cold wall is observed as compared to the hot wall. The temperature transients of pure thermal oil and nanotube-based nanofluids reached steady-state condition after 1–1.5 h. The surface corrected temperatures are calculated using the steady-state temperatures of the hot wall and cold wall. Figure 7 represents the corresponding changes in the temperature transients of the hot wall at different input heat flux. The temperature of the hot wall increases with the increase in input heat flux.

The steady-state temperatures for the hot wall, cold wall and the middle of the test cell for MWCNT-thermal oil-based nanofluid (1 mass%) at different input heat flux is shown in Fig. 8. It is observed that the hot wall temperature (at thermocouple position $x = 0$) increases with increasing input heat flux. Similar behavior is observed in nanofluid (at $x = 1.5$ cm). However, a mitigated increase in nanofluid temperature compared to the hot wall is observed with the increase in input heat flux. Similar behaviors are reported in previous studies by Ho et al. [28] and Putra et al. [27]. At the cold wall ($x = 3$ cm), a minute increase in temperature is observed as compared to the hot wall and the nanofluid which is attributed to the effective dissipation of heat from the enclosure at the cooling-side.

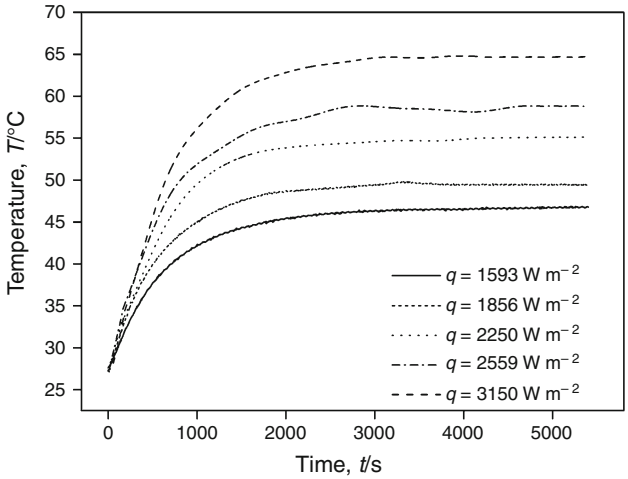


**Fig. 7** Temperature transients of MWCNT-thermal oil-based nanofluid (0.1 mass%) at the hot wall with different input heat flux

### Heat transfer experiments

The natural convection in nanofluids takes place due to the density difference and buoyancy forces. The particle distribution and the temperature gradient significantly affect

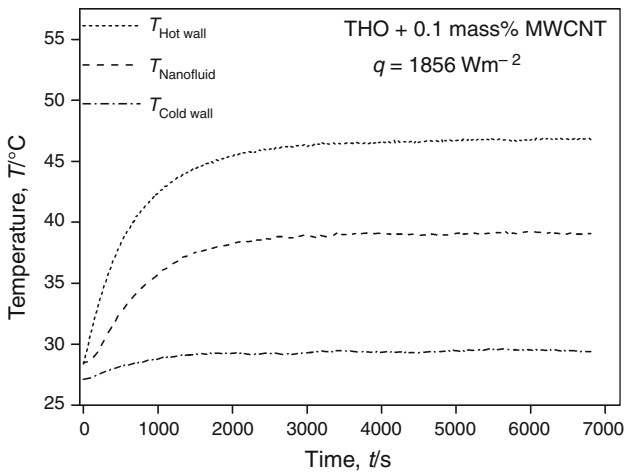


**Fig. 6** Temperature transients of MWCNT-thermal oil-based nanofluid (0.1 mass%) at an input heat flux of 1856 W $m^{-2}$

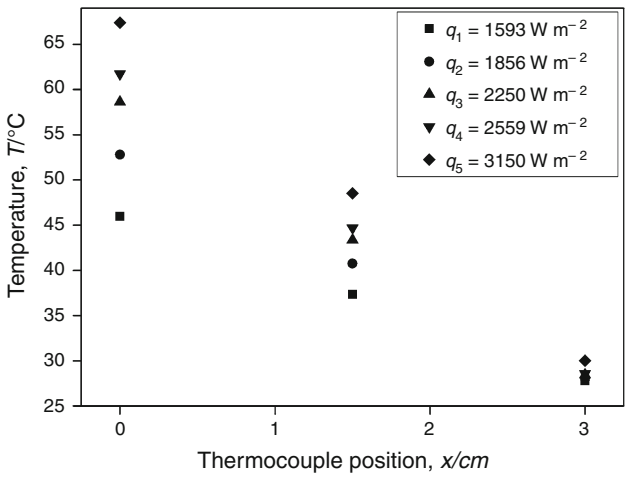


**Fig. 8** The steady-state temperatures of the hot wall, cold wall and nanofluid at different input heat flux for nanofluid at 1 mass% MWCNT

the buoyancy drive-natural convection. There are many factors which significantly affect natural convection behavior in nanofluids as compared to pure fluids. These factors include the role of slip mechanism between the nanoparticle and the base-fluid, the Brownian motion of nanoparticles, the uneven distribution of nanoparticles inside the base-fluid, Dufour effect and thermophoresis [17, 45–48]. In the present work, natural convection heat transfer characteristics of MWCNT-thermal oil-based nanofluids in rectangular enclosure with fixed aspect ratio are investigated. The temperature difference $\Delta T$ across hot and cold wall is measured and plotted against input power, shown in Fig. 9. A typical increasing trend is observed, the $\Delta T$ increases with an increase in input heat at the hot-side. It is found that with an increase in nanotube concentration in thermal oil, the $\Delta T$ across the hot and cold wall is increased. A significant rise in $\Delta T$ is observed at 1 mass% nanotube loading as compared to pure thermal oil. This outcome exhibits the poor performance of high concentrations of nanotube-thermal oil-based nanofluids for cooling applications by natural convection. The elevated $\Delta T$ for nanofluids compared to thermal oil may correspond to the additional resistance in heat transfer caused by the presence of nanotubes in thermal oil. This change is not significant at low input heat (7.65 W) for thermal oil and nanofluids. However, with the increase in input heat, the rise in $\Delta T$ becomes significant.

The heat transfer coefficient of pure thermal oil and nanofluids are estimated. The relative changes in heat transfer coefficient of nanofluids with respect to base-fluid are compared in Fig. 10. It is observed that all nanofluids showed deterioration in heat transfer coefficient. It is also observed that despite the higher thermal conductivity of the nanotubes-based nanofluids, the nanofluids showed poor

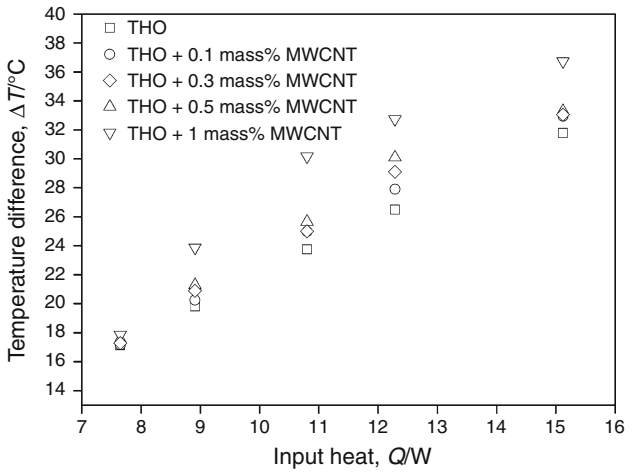


**Fig. 9** The temperature difference $\Delta T$ across hot and cold wall for thermal oil and MWCNT-thermal oil-based nanofluids at varying input heat

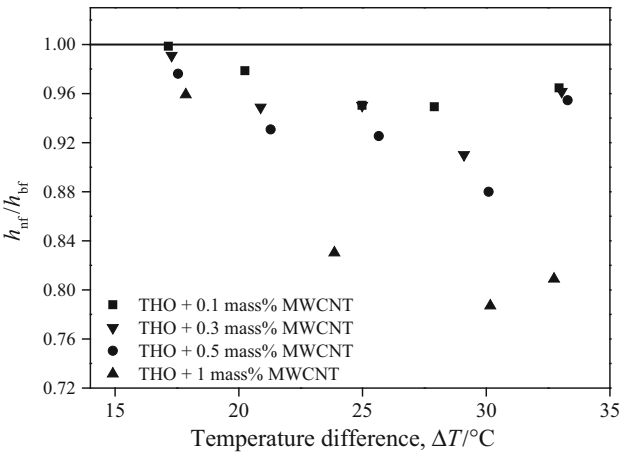


**Fig. 10** The relative heat transfer coefficient for nanofluids at different $\Delta T$ and nanotube concentrations

heat transfer performance for all concentrations. It is found that the heat transfer coefficient deteriorates further at higher concentrations of nanotubes as compared to thermal oil. The maximum deterioration of 21.3% is observed for 1 mass% nanotube concentration at $\Delta T$ = 30.16 °C.

Hwang et al. [49] investigated the natural convection heat transfer behavior in a rectangular enclosure heated from bottom. It was observed that the relative heat transfer coefficient increased with the increase in average temperature of $Al_2O_3$-water-based nanofluids. However, a contradictory behavior is observed for MWCNT-thermal oil-based nanofluids in the current study. The distribution of relative heat transfer coefficient with respect to temperature difference across the enclosure is not following any pattern. The relative heat transfer coefficient exhibits a decreasing trend at low $\Delta T$. However, at high values of $\Delta T$, the relative heat transfer coefficient is observed to be increasing again. This outcome is observed in all samples of nanofluids. This phenomenon might attribute to the particle–liquid interaction at different conditions and thermophysical properties especially thermal conductivity and viscosity of pure oil and nanofluids.

The kinetic theory of colloidal suspensions explains that the Brownian motion of nanoparticles increases with an increase in temperature, which increases the energy transfer due to intensified collisions among particles. However, at high concentration of nanoparticles in base-fluid, the packing effect is more prominent, and which decreases the Brownian motion of the nanoparticles thus increases the effective viscosity of nanofluid [50]. It is evident from Fig. 3 that the effective viscosity shoots up to 62% which can be the one of main reasons for deteriorating heat transfer behavior. The buoyancy-driven forces can be reduced at elevated viscosity of liquids and the heat transfer from hot-side to the cold-side can only be more

through conductive mode than convective mode of heat transfer as compared to the pure oil. Therefore, the observed deterioration in the heat transfer characteristics of MWCNTs-thermal oil-based nanofluids can be mainly attributed to the high viscosity of nanofluids. The effective viscosity of the nanofluid is found to be increasing with the increase in nanotube concentration, which could be the hindrance towards the convective heat transfer in the nanofluid.

It should be noted that the change in Nusselt number at different particle loadings signifies the mode of heat transfer only. The value of Nusselt number does not imply any improvement or the deterioration in heat transfer rate during convection process when the thermal conductivity varies with the nanoparticle concentration. However, the changes in overall heat transfer coefficient only represent the enhancement or deterioration on the overall heat transfer performance. The relative changes in Nusselt number of nanofluids with respect to pure thermal oil is estimated and presented in Fig. 11. It is observed that the addition of nanotubes in the thermal oil tends the nanofluids towards conductive-dominant heat transfer as compared to pure oil. The Nusselt number is decreasing by the increase in nanotube concentration. Similar trends were observed in previous studies for metal oxides-turbine oil- [26], $Al_2O_3$-water- [27] and $SiO_2$-water- [51] based nanofluids. The maximum reduction of 35.74% in relative Nusselt number is observed for 1 mass% nanotube loading at $\Delta T$ = 30.16 °C. This significant deterioration behavior is attributed to the increase in effective thermal conductivity of nanofluids. The changes in other thermophysical properties such as effective viscosity, effective density, effective specific heat capacity and effective coefficient of thermal expansion are also influential in the deterioration of heat transfer coefficient of this particular nanofluid.

The average Nusselt number for the MWCNT-thermal oil-based nanofluids at different Rayleigh number is plotted in Fig. 12. It is found that the nanofluid at all concentrations shows lower heat transfer enhancement compared to pure thermal oil. The Nusselt number decreases for nanofluids as compared to thermal oil. The maximum reduction is observed at 1 mass% nanotubes loading. A leftward shift in the Rayleigh number is observed for nanofluids. This left shift is more significant at higher concentrations of nanotubes in thermal oil. This is attributed to the significant changes in thermophysical properties of nanofluids at different temperatures and nanoparticle concentrations. Similar behavior was observed by Putra et al. [27] and Ho et al. [28] for $Al_2O_3$-water-based nanofluids.

The present work is compared with the existing literature [18], where *f*-$Al_2O_3$-thermal oil-based nanofluid was used to investigate heat transfer characteristics in the similar geometry and heat flux conditions. An increment in the heat transfer coefficient was found for *f*-$Al_2O_3$-thermal oil-based nanofluids as compared to the pure thermal oil. A maximum increment of 14% was observed for the highest concentration (3 mass%) of alumina in thermal oil. A comparative graph of the heat transfer coefficient ratio at varying nanoparticle concentrations is presented in Fig. 13. An opposite trend is evidently observed between both types of nanofluids. The alumina-based nanofluids exhibit an increase in heat transfer coefficient ratio with the increase in nanoparticle concentration, exhibiting an improved heat transfer behavior. Whereas, the nanotubes-based nanofluids illustrate decrement in heat transfer coefficient ratio with respect to particle concentration, demonstrating a considerable deterioration in heat transfer behavior. The comparative result clearly suggests that the heat transfer behavior of nanofluids does not necessarily depend only on

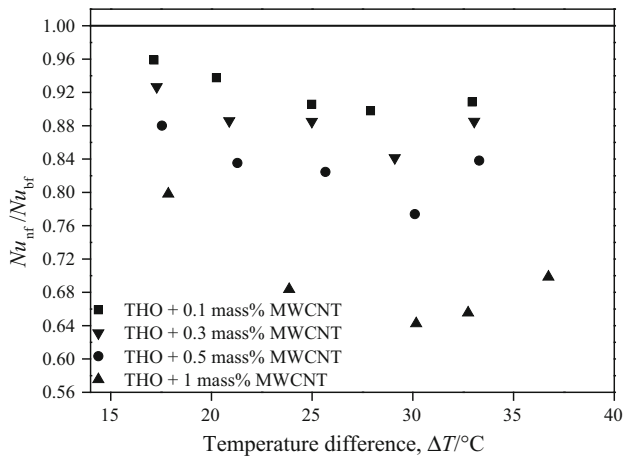


**Fig. 11** The relative Nusselt number for nanofluids at different $\Delta T$ and nanotube concentrations

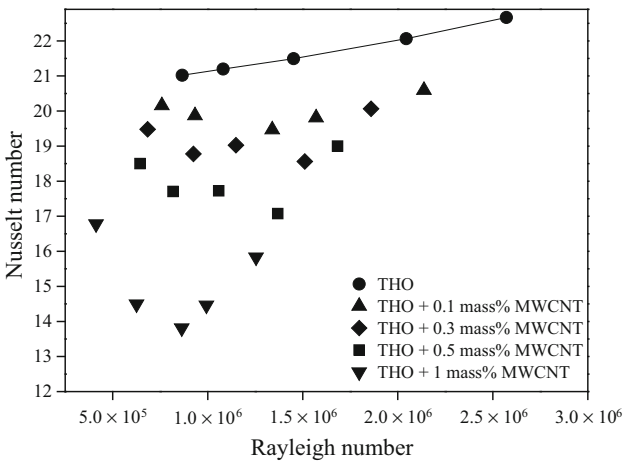


**Fig. 12** The average Nusselt number for MWCNT-thermal oil-based nanofluids at varying Rayleigh numbers

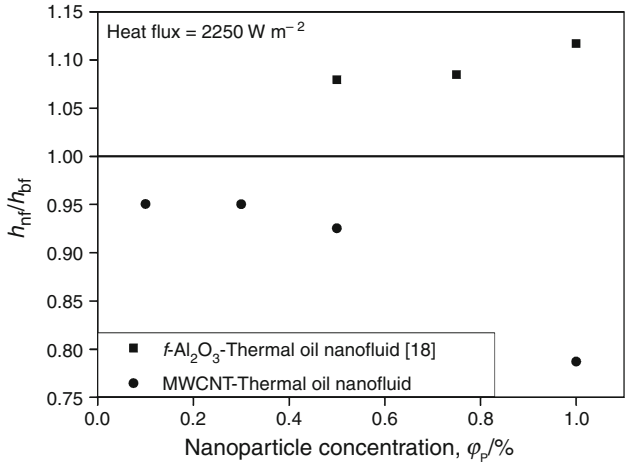


**Fig. 13** The comparison of the heat transfer coefficient ratio for *f*-$Al_2O_3$-thermal oil-based nanofluid [18] and the present work at similar heat flux condition (2250 W m$^{-2}$)

the thermal conductivity of nanofluids. The natural convection heat transfer characteristics depend on all thermophysical properties and interactions at the particle–liquid interface.

The change in interactions at the particle–liquid interface due to increase in temperature may affect the natural convection heat transfer behavior in nanofluids. The diffusiophoresis may take place when the nanoparticles move towards higher concentration zone from a lower concentration zone. Due to this movement of nanoparticles, the nanofluid tends toward agglomeration, which can significantly deteriorate the stability and overall heat transfer rate. The agglomeration in nanofluids can cause sedimentation of nanoparticles and many studies have reported the sedimentation of nanoparticles as one of the main reason for deteriorating heat-transfer [27, 29, 52–54]. It is also notable that the aforementioned phenomenon may differ for different nanofluid combinations. The deterioration or improvement in heat transfer behavior of nanofluids may differ because different types of nanoparticles exhibit different particle–liquid interactions. The high viscosity of nanofluids can influence the thermal and momentum boundary layer thickness which can diminish natural convection heat transfer characteristics.

## Uncertainty analysis

The relative uncertainty in the heat transfer parameters are estimated using Moffat method [55]. This widely used method has been reported in many investigations [26, 56–58]. The maximum precisions for the voltmeter, clamp ammeter and the thermocouple are ± 0.5 V, ± 0.0025 A and ± 0.1 °C, respectively. A measuring balance is used to prepare nanofluids, which has a precision of ± 0.0001 g. The maximum precision for the dimensions of rectangular enclosure is ± 0.5 mm. The maximum possible uncertainty for ammeter, voltmeter, measuring balance, thermocouple, and size of the enclosure can be calculated by dividing the maximum precision with the minimum experimental value. For instance, the maximum possible uncertainty for ammeter is

$$E_{\mathrm{I}} = \pm 0.0025/0.17 = \pm 0.0147.$$

The maximum possible uncertainty for the average heat transfer coefficient $E_{\mathrm{h,\,max}}$ is given in Eq. 11. The corresponding maximum possible uncertainty in the heat transfer coefficient is estimated to be ± 3.88%. Similarly, the maximum uncertainty in Nusselt number and Rayleigh number is found to be ± 4.22 and ± 5.08%, respectively.

$$E_{\mathrm{h,\,max}} = \pm\sqrt{(E_{\mathrm{V}})^2 + (E_{\mathrm{I}})^2 + (-E_{\mathrm{T_H - T_C}})^2 + (-E_{\mathrm{A}})^2 + (E_{\mathrm{MB}})^2} \quad (11)$$

## Conclusions

The natural convection heat transfer behavior in MWCNT-thermal oil-based nanofluids are investigated at varying concentrations up to 1 mass% and input heat flux up to 3150 W m$^{-2}$ at fixed aspect ratio of 4. The temperature transients are recorded for each sample and it is found that the nanotube-thermal oil-based nanofluids showed higher $\Delta T$ compared to pure thermal oil. The average heat transfer coefficient and the average Nusselt number deteriorated up to 21.3 and 35.74%, respectively, at for 1 mass% nanofluid. The results suggest that, despite higher thermal conductivities of nanofluids, the nanofluids showed poor heat transfer behavior during natural convection. This is attributed to the relative changes in thermophysical properties of nanofluids especially effective viscosity of nanofluids which shoots up to 62% at 1 mass% MWCNT-based nanofluid. The involvement of other factors, such as role of particle–liquid slip, diffusiophoresis, degree of agglomeration and packing effects might contribute to the deteriorating behavior of nanofluids. Based on the present results, the dispersions of MWCNT nanoparticle in thermal oil is not suitable for the natural convection heat transfer process at studied concentration of nanofluids. However, future experimental studies can be performed to investigate the suitability of nanofluids in forced convection.

**Acknowledgements** This work is supported by Chemical Engineering Department of Universiti Teknologi PETRONAS. The financial assistance is provided by YUTP 0153AA-E28.

## References


1. Bahiraei M, Hangi M, Saeedan M. A novel application for energy efficiency improvement using nanofluid in shell and tube heat exchanger equipped with helical baffles. Energy. 2015;93:2229–40.
2. Hussien AA, Abdullah MZ, Al-Nimr MDA. Single-phase heat transfer enhancement in micro/minichannels using nanofluids: theory and applications. Appl Energy. 2016;164:733–55.
3. Shariatmadar FS, Pakdehi SG. Synthesis and characterization of aviation turbine kerosene nanofuel containing boron nanoparticles. Appl Therm Eng. 2017;112:1195–204.
4. Ghaderian J, Sidik NAC, Kasaeian A, Ghaderian S, Okhovat A, Pakzadeh A, Samion S, Yahya WJ. Performance of copper oxide/distilled water nanofluid in evacuated tube solar collector (ETSC) water heater with internal coil under thermosyphon system circulations. Appl Therm Eng. 2017;121:520–36.
5. Toghraie D, Chaharsoghi VA, Afrand M. Measurement of thermal conductivity of ZnO–$TiO_2$/EG hybrid nanofluid. J Therm Anal Calorim. 2016;125:527–35.
6. Bashirnezhad K, Ghavami M, Alrashed AAAA. Experimental investigations of nanofluids convective heat transfer in different flow regimes: a review. J Mol Liq. 2017;244:309–21.
7. Ilyas SU, Pendyala R, Marneni N. Preparation, sedimentation, and agglomeration of nanofluids. Chem Eng Technol. 2014;37:2011–21.
8. Raei B, Shahraki F, Jamialahmadi M, Peyghambarzadeh SM. Experimental study on the heat transfer and flow properties of γ-$Al_2O_3$/water nanofluid in a double-tube heat exchanger. J Therm Anal Calorim. 2017;127:2561–75.
9. Afshari A, Akbari M, Toghraie D, Yazdi ME. Experimental investigation of rheological behavior of the hybrid nanofluid of MWCNT–alumina/water (80%)–ethylene-glycol (20%). J Therm Anal Calorim. 2018;132:1001–15.
10. Pendyala R, Ilyas SU, Lim LR, Marneni N. CFD analysis of heat transfer performance of nanofluids in distributor transformer. Proc Eng. 2016;148:1162–9.
11. Kasaeipoor A, Malekshah EH, Kolsi L. Free convection heat transfer and entropy generation analysis of MWCNT-MgO (15%–85%)/Water nanofluid using Lattice Boltzmann method in cavity with refrigerant solid body-experimental thermo-physical properties. Powder Technol. 2017;322:9–23.
12. Kolsi L, Mahian O, Öztop HF, Aich W, Borjini MN, Abu-Hamdeh N, Aissia HB. 3D buoyancy-induced flow and entropy generation of nanofluid-filled open cavities having adiabatic diamond shaped obstacles. Entropy. 2016;18:232.
13. Estellé P, Mahian O, Maré T, Öztop HF. Natural convection of CNT water-based nanofluids in a differentially heated square cavity. J Therm Anal Calorim. 2017;128:1765–70.
14. Rashidi S, Eskandarian M, Mahian O, Poncet S. Combination of nanofluid and inserts for heat transfer enhancement. J Therm Anal Calorim. 2018. https://doi.org/10.1007/s10973-018-7070-9.
15. Rahimi A, Kasaeipoor A, Malekshah EH, Kolsi L. Experimental and numerical study on heat transfer performance of three-dimensional natural convection in an enclosure filled with DWCNTs-water nanofluid. Powder Technol. 2017;322:340–52.
16. Kolsi L, Lajnef E, Aich W, Alghamdi A, Aichouni MA, Borjini MN, Aissia HB. Numerical investigation of combined buoyancy-thermocapillary convection and entropy generation in 3D cavity filled with $Al_2O_3$ nanofluid. Alex Eng J. 2017;56:71–9.
17. Narahari M, Raju SSK, Pendyala R, Pop I. Transient two-dimensional natural convection flow of a nanofluid past an isothermal vertical plate using Buongiorno's model. Int J Numer Method Heat Fluid Flow. 2017;27:23–47.
18. Ilyas SU, Pendyala R, Narahari M. An experimental study on the natural convection heat transfer in rectangular enclosure using functionalized alumina-thermal oil-based nanofluids. App Therm Eng. 2017;127:765–75.
19. Trisaksri V, Wongwises S. Critical review of heat transfer characteristics of nanofluids. Renew Sustain Energy Rev. 2007;11:512–23.
20. Hu Y, He Y, Qi C, Jiang B, Schlaberg HI. Experimental and numerical study of natural convection in a square enclosure filled with nanofluid. Int J Heat Mass Transf. 2014;78:380–92.
21. Mahrood MRK, Etemad SG, Bagheri R. Free convection heat transfer of non Newtonian nanofluids under constant heat flux condition. Int Commun Heat Mass Transf. 2011;38:1449–54.
22. Li H, He Y, Hu Y, Jiang B, Huang Y. Thermophysical and natural convection characteristics of ethylene glycol and water mixture based ZnO nanofluids. Int J Heat Mass Transf. 2015;91:385–9.
23. Beheshti A, Shanbedi M, Heris SZ. Heat transfer and rheological properties of transformer oil-oxidized MWCNT nanofluid. J Therm Anal Calorim. 2014;118:1451–60.
24. Amiri A, Kazi SN, Shanbedi M, Zubir MNM, Yarmand H, Chew BT. Transformer oil based multi-walled carbon nanotube-hexylamine coolant with optimized electrical, thermal and rheological enhancements. RSC Adv. 2015;5:107222–36.
25. Thomas S., Sobhan CB, Taha-Tijerina J, Narayanan TN, Ajayan PM. Investigations on transient natural convection in boron nitride-mineral oil nanofluid systems, ASME international mechanical engineering congress and exposition, vol 9: Micro- and nano-systems engineering and packaging, parts A and B (2012); 671–678. https://doi.org/10.1115/imece2012-87420.
26. Heris SZ, Pour MB, Mahian O, Wongwises S. A comparative experimental study on the natural convection heat transfer of different metal oxide nanopowders suspended in turbine oil inside an inclined cavity. Int J Heat Mass Transf. 2014;73:231–8.
27. Putra N, Roetzel W, Das SK. Natural convection of nano-fluids. Heat Mass Transf. 2003;39:775–84.
28. Ho CJ, Liu WK, Chang YS, Lin CC. Natural convection heat transfer of alumina-water nanofluid in vertical square enclosures: an experimental study. Int J Therm Sci. 2010;49:1345–53.
29. Kouloulias K, Sergis A, Hardalupas Y. Sedimentation in nanofluids during a natural convection experiment. Int J Heat Mass Transf. 2016;101:1193–203.
30. Wen D, Ding Y. Formulation of nanofluids for natural convective heat transfer applications. Int J Heat Fluid Flow. 2005;26:855–64.
31. Nnanna AG. Experimental model of temperature-driven nanofluid. J Heat Transf. 2006;129:697–704.
32. Ni R, Zhou S-Q, Xia K-Q. An experimental investigation of turbulent thermal convection in water-based alumina nanofluid. Phys Fluids. 2011;23:022005.
33. Li CH, Peterson GP. Experimental studies of natural convection heat transfer of $Al_2O_3$/DI water nanoparticle suspensions (nanofluids). Adv Mech Eng. 2010;2:742739.
34. Choudhary R, Subudhi S. Aspect ratio dependence of turbulent natural convection in $Al_2O_3$/water nanofluids. Appl Therm Eng. 2016;108:1095–104.
35. Xing M, Yu J, Wang R. Experimental investigation and modelling on the thermal conductivity of CNTs based nanofluids. Int J Therm Sci. 2016;104:404–11.
36. Ilyas SU, Pendyala R, Narahari M. Stability and thermal analysis of MWCNT-thermal oil-based nanofluids. Colloids Surf A. 2017;527:11–22.
37. Ilyas SU, Pendyala R, Narahari M. Stability of Nanofluids. In: Korada VS, Hisham BHN, editors. Engineering applications of nanotechnology: from energy to drug delivery. Cham: Springer; 2017. p. 1–31.

38. Ilyas SU, Pendyala R, Narahari M. Stability and agglomeration of alumina nanoparticles in ethanol-water mixtures. Proc Eng. 2016;148:290–7.
39. Pak BC, Cho YI. Hydrodynamic and heat transfer study of dispersed fluids with submicron metallic oxide particles. Exp Heat Transf. 1998;11:151–70.
40. Bayat J, Nikseresht AH. Thermal performance and pressure drop analysis of nanofluids in turbulent forced convective flows. Int J Therm Sci. 2012;60:236–43.
41. Ilyas SU, Pendyala R, Shuib A, Marneni N. A review on the viscous and thermal transport properties of nanofluids. Adv Mater Res. 2014;917:18–27.
42. Sridhara V, Satapathy LN. Effect of nanoparticles on thermal properties enhancement in different oils—a review. Crit Rev Solid State. 2015;40:399–424.
43. Bashirnezhad K, Bazri S, Safaei MR, Goodarzi M, Dahari M, Mahian O, Dalkılıça AS, Wongwises S. Viscosity of nanofluids: a review of recent experimental studies. Int Commun Heat Mass Transf. 2016;73:114–23.
44. Ilyas SU, Pendyala R, Narahari M, Susin L. Stability, rheology and thermal analysis of functionalized alumina- thermal oil-based nanofluids for advanced cooling systems. Energ Convers Manag. 2017;142:215–29.
45. Pakravan HA, Yaghoubi M. Combined thermophoresis, Brownian motion and Dufour effects on natural convection of nanofluids. Int J Therm Sci. 2011;50:394–402.
46. Tzou DY. Thermal instability of nanofluids in natural convection. Int J Heat Mass Transf. 2008;51:2967–79.
47. Bahiraei M. Particle migration in nanofluids: a critical review. Int J Therm Sci. 2016;109:90–113.
48. Mahdavi M, Sharifpur M, Meyer JP. Simulation study of convective and hydrodynamic turbulent nanofluids by turbulence models. Int J Therm Sci. 2016;110:36–51.
49. Hwang KS, Lee J-H, Jang SP. Buoyancy-driven heat transfer of water-based $Al_2O_3$ nanofluids in a rectangular cavity. Int J Heat Mass Transf. 2007;50:4003–10.
50. Mewis J, Wagner NJ. Colloidal suspension rheology. Cambridge: Cambridge University Press; 2012.
51. Mahian O, Kianifar A, Heris SZ, Wongwises S. Natural convection of silica nanofluids in square and triangular enclosures: theoretical and experimental study. Int J Heat Mass Transf. 2016;99:792–804.
52. Ashrafmansouri S-S, Esfahany MN. Mass transfer in nanofluids: a review. Int J Therm Sci. 2014;82:84–99.
53. Khanafer K, Vafai K, Lightstone M. Buoyancy-driven heat transfer enhancement in a two-dimensional enclosure utilizing nanofluids. Int J Heat Mass Transf. 2003;46:3639–53.
54. Meng X, Zhang X, Li Q. Numerical investigation of nanofluid natural convection coupling with nanoparticles sedimentation. Appl Therm Eng. 2016;95:411–20.
55. Moffat RJ. Describing the uncertainties in experimental results. Exp Therm Fluid Sci. 1988;1:3–17.
56. Pendyala R, Jayanti S, Balakrishnan AR. Flow and pressure drop fluctuations in a vertical tube subject to low frequency oscillations. Nucl Eng Des. 2008;238:178–87.
57. Pendyala R, Jayanti S, Balakrishnan AR. Convective heat transfer in single-phase flow in a vertical tube subjected to axial low frequency oscillations. Heat Mass Transf. 2008;44:857–64.
58. Heris SZ, Edalati Z, Noie SH, Mahian O. Experimental investigation of $Al_2O_3$/water nanofluid through equilateral triangular duct with constant wall heat flux in laminar flow. Heat Transf Eng. 2013;35:1173–82.